

Effects of Antimony Doping and Sintering Atmosphere on the Properties of $K_4CuNb_8O_{23}$ Modified $K_{0.5}Na_{0.5}NbO_3$ (KNN-KCN) Lead-free Piezoceramics

Murat MURUTOĞLU¹, Erdem AKÇA², Hüseyin YILMAZ¹

¹Gebze Technical University, Department of Materials Science and Engineering, TURKEY

²Sivas Cumhuriyet University, Department of Metallurgical and Materials Engineering, TURKEY

Sorumlu Yazar / Corresponding Author

Murat MURUTOĞLU
m.murutoglu@gtu.edu.tr

Makale Bilgisi / Article Info

Sunulma / Received : 19.04.2021

Düzeltilme / Revised : 12.06.2021

Kabul / Accepted : 13.06.2021

Anahtar Kelimeler

Kurşunsuz Piezoseramikler
Sinterleme
Katılama
Dielektrik Özellikler

Keywords

Lead-free Piezoceramics
Sintering
Doping
Dielectric Properties

Abstract

For high power applications, the effects of dopant, sintering atmosphere and time on the electrical properties of environmentally friendly lead-free KNN-KCN piezoceramics were investigated. 3 %mol Sb doped KNN-KCN ceramics were sintered in air and oxygen atmosphere for 2, 4 and 6 hours, and their electrical properties were compared to the undoped ones prepared under identical conditions. With Sb doping, the piezoelectric charge coefficient d_{33} (~100 pC/N) and the dielectric constant (~520, at room temperature and at 10kHz) values were increased considerably. It was found that the densities of doped and undoped KNN-KCN ceramics sintered in the oxygen atmosphere increased by ~1.5 %, and dielectric losses ($\tan\delta$) decreased by approximately 30-35 %. Cole-Cole analyses of ceramics were done by impedance spectroscopy. Although Sb doping decreased impedance values, it was found to increase when sintered in the oxygen atmosphere.

Antimon Katılama ve Sinterleme Atmosferinin $K_4CuNb_8O_{23}$ ile Modifiye edilmiş $K_{0.5}Na_{0.5}NbO_3$ (KNN-KCN) Kurşunsuz Piezoseramiklerin Özelliklerine Etkileri

Özet

Yüksek güç uygulamaları için, çevre dostu kurşunsuz KNN-KCN piezoseramiklerin elektriksel özellikleri üzerine katılamanın, sinterleme atmosferinin ve zamanın etkileri araştırılmıştır. %3 mol Sb katılı KNN-KCN seramikleri hava ve oksijen atmosferinde 2, 4 ve 6 saat sinterlenmiş ve elektriksel özellikleri aynı koşullarda hazırlanan katısız seramiklerle karşılaştırılmıştır. Sb katılama ile piezoelektrik yük katsayısı d_{33} (~100 pC/N) ve dielektrik sabiti (~520, 10 kHz'de ve oda sıcaklığında) değerleri önemli ölçüde artırılmıştır. Oksijen atmosferinde sinterlenen katılı ve katısız KNN-KCN seramiklerinin yoğunluklarının ~% 1,5 arttığı ve dielektrik kayıplarının ($\tan\delta$) yaklaşık %30-35 oranında azaldığı tespit edilmiştir. Seramiklerin Cole-Cole analizleri empedans spektroskopisi ile yapılmıştır. Sb katısının empedans değerlerini düşürmesine rağmen oksijen atmosferinde sinterlendiğinde arttığı görülmüştür.

1. INTRODUCTION

The remarkable ferroelectric and piezoelectric properties of $\text{Pb}[\text{Zr}_{(x)}\text{Ti}_{(1-x)}]\text{O}_3$ (PZT) has triggered researches to find new candidate lead-based perovskite materials since 1950s. Some binary ceramic systems with high performances such as $\text{Pb}(\text{Zn}_{1/3}\text{Nb}_{2/3})\text{O}_3\text{-PbTiO}_3$ (PZN–PT), $\text{Pb}(\text{Mg}_{1/3}\text{Nb}_{1/3})\text{O}_3\text{-PbTiO}_3$ (PMN–PT) and $\text{Pb}(\text{Ni}_{1/3}\text{Nb}_{1/3})\text{O}_3\text{-Pb}(\text{Zr,Ti})\text{O}_3$ (PNN–PZT) have been found thanks to great efforts focused on that issue¹⁻⁵. Lead-based ceramics with outstanding piezoelectric and ferroelectric properties have been extensively used in civil and military applications as sensor, transducer, actuator, etc. since then^{4,5}. However, the presence of the toxic lead (Pb), which may be up to 60 % by weight, was considered problematic due to the health and environmental concerns formed over the time^{6,7}. Especially, the European Union and some other governments have restricted the use of lead in electronic devices except the ones used in military and space industries since the beginning of 2000s⁸⁻¹⁰. Thereby, the studies on alternative lead-free piezoceramics have increased exponentially over the years due to these restrictions.

Due to their relatively high electrical properties and high Curie temperature (around 420 °C), $(\text{K}_{0.5}\text{Na}_{0.5})\text{NbO}_3$ (KNN)-based systems were considered one of the most promising lead-free piezoelectric ceramic candidates with perovskite structure¹¹. However, it was very difficult to control the microstructure and to maintain the stoichiometry at the same time due to the volatility of alkali elements even at low temperatures in the pure KNN ceramics^{12,13}. Alkali volatilization not only deteriorated the sinterability of it but also resulted in poor electrical and electromechanical properties^{12,14}. To solve the as mentioned problems, sintering of KNN ceramics was usually carried out with sintering additives and dopants. For instance, several reports have showed that the incorporation of $\text{K}_4\text{CuNb}_8\text{O}_{23}$ (KCN) into KNN not only increased the densification behavior but also induced hard electrical character, which turned out to be a very important requirement to be eligible for high-power ultrasonic applications, like ultrasonic cleaning, cutting, drilling, welding, forming, machining, etc.¹⁵⁻¹⁷. On the other hand, a high electrical ($Q_e=1/\tan\delta$) and a mechanical quality factor (Q_m) together with a low piezoelectric property is considered unique to electrically hard piezoceramics due to the inhibition of domain wall motion by pinning of it with acceptor-oxygen vacancy defect dipoles¹⁵⁻²¹. Enhancing in the piezoelectric performance was also achieved through compositionally engineering it with co-doping^{16,17}. In the literature, it was reported that sintering of the KNN-based ceramics in an oxygen-rich atmosphere improved densification as well as the ferroelectric properties^{22,23}. A similar improvement in the properties was also achieved by doping Sb into KNN-based ceramics^{24,25}.

In this study, sintering behavior of KCN modified KNN piezoceramics were studied as a function of doping, sintering atmosphere and time to further improve their electrical properties. Undoped and Sb doped KNN-KCN ceramics were sintered for 2, 4 or 6 hours in air or oxygen atmosphere.

In sintering at oxygen atmosphere, the possible use of KNN ceramics for high power ultrasonic applications by reducing the dielectric losses via controlling the defect chemistry was aimed.

2. PROCEDURE

K_2CO_3 (Merck, 99%), Na_2CO_3 (Merck, 99%), Nb_2O_5 (Alfa Aesar, 99.5%), Sb_2O_5 (BDH, 99.9%) and CuO (Merck, 96%) powders were used as starting raw materials to synthesize neat and 3 mol% Sb doped KNN-KCN ceramics. Initially, undoped $(\text{K}_{0.5}\text{Na}_{0.5})\text{NbO}_3$ (KNN), 1.5 % mol Sb_2O_5 doped $(\text{K}_{0.5}\text{Na}_{0.5}\text{Nb}_{0.97}\text{Sb}_{0.03})\text{O}_3$ (KNN-Sb) and $\text{K}_4\text{CuNb}_8\text{O}_{23}$ (KCN) were synthesized by solid state calcination as intermediate powders. K_2CO_3 and Na_2CO_3 were kept in a drying oven at 200 °C for 24 h before being using due to the hygroscopic nature of them. Stoichiometric amount of powders was weighed and added to the 125 ml high density polyethylene Nalgene bottles and were milled for 24 h at 140 rpm using 3 and 5 mm yttria stabilized zirconia milling media in ethanol solvent. Then, KCN and KNN powders were calcined for 2 h at 600°C and 700°C, respectively. Each calcined powder was milled one more time. 0.5 mol% KCN powders as sintering aid were then added to each synthesized KNN and KNN-Sb powders separately before mixing them with polymeric binder solution, which was prepared by dissolving fish oil (Sigma-Aldrich), polyvinyl butyral (Sigma-Aldrich) and dioctyl phthalate (Sigma-Aldrich) in ethanol. After ball milling and drying the powders were sieved through a 90 µm stainless steel sieve. Pellets were pressed in a 12.45 mm diameter steel die before being isostatically cold pressed at 200 MPa. The binder burn-out process was carried out isothermally by holding first at 275 °C and then at 600 °C for one hour, each. Heating rate was kept constant at 1 °C/min. After that the pellets were sintered at 1100 °C for 2, 4 or 6 h in air or oxygen atmospheres with 5 °C/min heating and 10 °C/min cooling rates. All samples were sintered on a sacrificial KNN powder bed in an Al_2O_3 crucible to compensate for the possible alkali evaporation at high temperature and also prevent the reaction of the samples with the alumina crucible. The Archimedes' method was used to determine the densities of sintered samples. Before doing electrical characterizations, parallel surfaces of the disc shaped samples were polished and then silver paste was applied as electrode and were fired at 600 °C for 30 minutes. The samples were poled at 120 °C in a silicon oil bath by applying a DC electric field of 50 kV/cm for 15 min.^{15,16} Piezoelectric properties were measured using a Berlincourt d_{33} -meter (Sinocera, YE2730A) after 24 hours of waiting. The temperature dependence of dielectric constant (ϵ_r) and dielectric loss ($\tan\delta$) values were measured at 1 kHz, 10 kHz, 100 kHz and 1 MHz with an LCR meter (Hioki-3532-50) between 25 and 500 °C with a heating rate of 2 °C/min.

X-ray diffractometer (XRD) (Rigaku D/max–2200) using $\text{CuK}\alpha$ ($\lambda = 1.5405$ Å) radiation was used to examine the phase structure of sintered KNN ceramic pellets. Microstructural analysis from fractured surfaces of samples was performed by using a scanning electron microscope (SEM) device (Philips XL 30 SFEG). Impedance vs temperature measurements were carried out via an impedance analyzer (Keysight E4990A) in the temperature range of 425 to 525 °C and frequency range of 100 Hz to 10 MHz.

3. FINDINGS and DISCUSSION

Fig. 1 shows that XRD patterns of KNN-KCN and KNN-KCN-Sb ceramics sintered at 1100 °C for 2, 4 and 6 h and in air or oxygen

atmospheres. Perovskite structure with orthorhombic symmetry mixed with minor phases were obtained in all ceramics. The (002), (200) and (020) peak splitting around $2\theta \approx 44.5\text{--}46.5^\circ$ indicated that the structure was orthorhombic as expected.

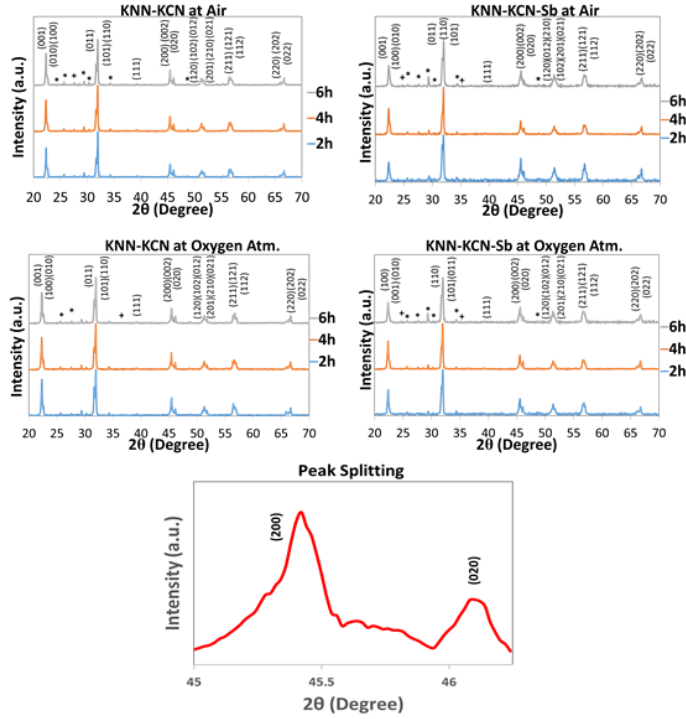


Figure 1. XRD patterns of KNN-KCN and KNN-KCN-Sb ceramics sintered at 1100 °C for 2, 4 and 6 h and in air or oxygen atmospheres with peak splitting at $2\theta \approx 44.5\text{--}46.5^\circ$.

KCN phases marked with asterisk (*) were identified in the XRD patterns. Matsubara et al reported that when the amount of KCN in the KNN system were higher than 0.4 mol%, the KCN phase could be distinguished in the X-ray diffraction patterns²⁰. In addition, other minor amount of secondary phase(s), marked with plus sign (+), as seen on the XRD patterns of the samples sintered for 6 h probably existed due to the prolonged sintering dwell time. No other significant differences in the XRD patterns were detected related to the air or oxygen sintering atmosphere.

Fig. 2 (a)–(l) shows the SEM micrograph taken from the fracture surface of KNN-KCN and KNN-KCN-Sb ceramics, sintered at 1100 °C for different sintering periods, namely 2, 4 and 6 h, and atmospheres (air or oxygen). The images revealed a transgranular fracture mode in these ceramics probably due to the melting and segregation of KCN additive to the grain boundaries²⁰. Grain sizes less than 2 μm were typical in these micrographs with faceted grains consistent with the findings in the literature^{17,26,27}.

Table 1 shows the relative theoretical densities of KNN-KCN and KNN-KCN-Sb ceramics as a function of sintering time and atmosphere, in which the theoretical density of KNN-KCN was taken as 4.51 g/cm³. It was found that the relative densities of the samples did not change much with the sintering time.

Table 1. Relative densities of samples sintered at different conditions.

ρ [%]	KNN-KCN Sintering Atmosphere		KNN-KCN-Sb Sintering Atmosphere	
	Air	Oxygen	Air	Oxygen
Sintering time				
2 h	98.1	99.2	98.1	99.4
4 h	98.2	99.6	98.4	98.1
6 h	98.2	99.1	98.6	98.8

However, it was known that sintering in an oxygen atmosphere resulted in increased densities in KNN ceramics due to the prevention of grain growth^{22,23}. In addition to that, KCN promoted the densification of KNN since the copper-rich KCN behaved as liquid phase former and it made the A/B site ratio in the perovskite less than one^{20,28}. It was also found that the density of KNN-KCN system did not vary with Sb doping. However, the measured relative densities of both KNN-KCN and KNN-KCN-Sb ceramics sintered in an oxygen atmosphere were slightly higher than those of the ones sintered in air.

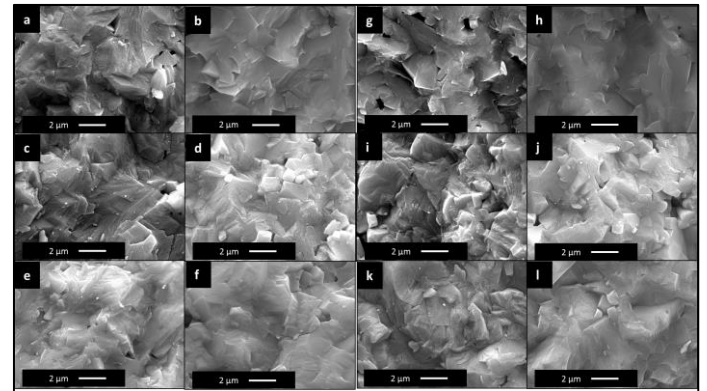


Figure 2. SEM images of KNN-KCN (a-b) 2h in air and oxygen atmosphere (c-d) 4h in air and oxygen atmosphere (e-f) 6h in air and oxygen atmosphere and KNN-KCN-Sb (g-h) 2h in air and oxygen atmosphere (i-j) 4h in air and oxygen atmosphere (k-l) 6h in air and oxygen atmosphere.

Table 2 lists the piezoelectric constant d_{33} values of KNN-KCN and KNN-KCN-Sb ceramics. Several different factors were found to affect the piezoelectric charge coefficient in KNN-KCN based ceramics. The d_{33} values were found to be more or less independent of the sintering time and/or sintering atmosphere for both of KNN-KCN and KNN-KCN-Sb ceramics.

Table 2. Piezoelectric constant d_{33} of samples sintered at different conditions.

d_{33} [pC/N]	KNN-KCN Sintering Atmosphere		KNN-KCN-Sb Sintering Atmosphere	
	Air	Oxygen	Air	Oxygen
Sintering time				
2 h	81	86	104	96
4 h	83	85	102	100
6 h	78	83	96	93

However, considerable enhancement in the d_{33} values stood out in the presence of Sb doping. Higher d_{33} values were observed by inducing a soft character due the high electronegativity of Sb^{5+} ions, as expected²⁴. Another contribution of Sb doping was the increase in the density, which was consistent with the reported results in previous works²⁵.

Table 3 (a)-(b) shows the relative dielectric constant (ϵ_r) and dielectric loss ($\tan\delta$) values, measured at 1, 10 100 kHz frequencies at room temperature from unpoled KNN-KCN and KNN-KCN-Sb ceramics sintered in air or oxygen atmosphere for 2 h, 4 h or 6 h. The average dielectric constant and dielectric loss values were found to be ~ 420 and $\sim 0.5\%$ for all KNN-KCN ceramics, respectively, while those values were found to be ~ 520 and $\sim 2\%$ for KNN-KCN-Sb ones, respectively.

Table 3. Room temperature relative dielectric constant (ϵ_r) and dielectric loss ($\tan\delta$) of samples sintered at different conditions.

KNN-KCN						
(a)	2 h		4 h		6 h	
Freq	Air	Oxy.	Air	Oxy.	Air	Oxy.
1 kHz	433	433	419	405	403	402
	% 0.44	% 0.38	% 0.44	% 0.37	% 0.45	% 0.31
10 kHz	430	430	416	403	401	400
	% 0.49	% 0.47	% 0.52	% 0.41	% 0.47	% 0.39
100 kHz	427	427	413	401	398	397
	% 0.70	% 0.63	% 0.75	% 0.58	% 0.66	% 0.58

KNN-KCN-Sb						
(b)	2 h		4 h		6 h	
Freq	Air	Oxy.	Air	Oxy.	Air	Oxy.
1 kHz	565	521	515	520	510	528
	% 2.1	% 1.3	% 1.9	% 1.4	% 2.4	% 1.5
10 kHz	548	510	502	508	495	516
	% 2.4	% 1.7	% 2.1	% 1.8	% 2.2	% 1.7
100 kHz	527	497	485	494	478	503
	% 3.2	% 2.3	% 2.7	% 2.4	% 2.8	% 2.4

Increases in dielectric constant and loss values for KNN-KCN-Sb were attributed to the softening of KNN-KCN system due to Sb doping. It was known that the substitution of a smaller Sb^{5+} ions for Nb^{5+} ions at the B-site in the perovskite structure results in increased off centering of B-site cation together with increased covalent character in bonding due to a shorter and stronger Sb-O bonding than Nb-O bonding^{24,25,29}. On the other hand, lower relative dielectric constant and dielectric loss values for all KNN-KCN ceramics were mainly related to the hardening of KNN because of the substitution of Cu^{2+} ions for Nb^{5+} ions resulting in increased amount of oxygen vacancies responsible for hindering domain wall motion, which is called the “pinning effect”^{15-20,30}. The effect of the sintering atmosphere on the dielectric constants was ambiguous for KNN-KCN and KNN-KCN-Sb ceramics, whereas dielectric loss values decreased considerably as a result of sintering in the oxygen atmosphere. It could be attributed to the reduction of space charges (electron, hole, etc.) by sintering in an oxygen atmosphere^{31,32}. Besides, it was also found that dielectric loss values were virtually insensitive to sintering time for all samples irrespective to the sintering atmospheres. Relative dielectric constants exhibited a decreasing tendency with increasing sintering time for KNN-KCN ceramics while no tendency was observed for KNN-KCN-Sb.

Fig 3 shows that the temperature dependence of ϵ_r and $\tan\delta$ from poled KNN-KCN and KNN-KCN-Sb ceramics sintered for 2h in air or oxygen atmosphere, measured at different frequencies on heating. It was clearly seen that two dielectric anomalies existed corresponding to the phase transitions, which were orthorhombic-tetragonal ($T_{O \rightarrow T}$) and tetragonal-cubic (Curie temperature, T_C) as shown in Fig 3. Orthorhombic to tetragonal and tetragonal to cubic phase transitions were found to be $\sim 195^\circ C$ and $\sim 230^\circ C$ for KNN-KCN and $\sim 365^\circ C$ and $\sim 415^\circ C$ for KNN-KCN-Sb ceramics, respectively. It was also found that sintering in an oxygen rich atmosphere had no significant effect on transition temperatures both on KNN-KCN and KNN-KCN-Sb ceramics.

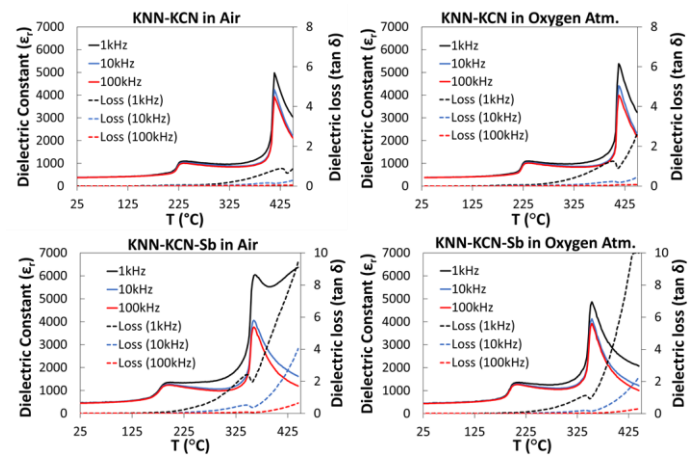
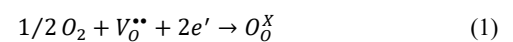


Figure 3. Temperature dependence of ϵ_r and $\tan\delta$ of poled KNN-KCN and KNN-KCN-Sb ceramics sintered for 2h at air or oxygen atmosphere, measured at different frequencies.

However, Sb doping has lowered not only the $T_{O \rightarrow T}$ but also the T_C of KNN-KCN ceramics as expected^{24,25,29}. This was explained in several reports as, when small ionic radius Sb^{5+} ions substituted Nb^{5+} ions in the B sites the resulting physical stresses and shrinkage in the lattice might stabilize the phases at lower temperatures^{24,29}. It should be noted that the working temperature of KNN-KCN ceramics was limited up to orthorhombic to tetragonal transition temperature^{15,18}. The higher phase transition temperature meant that the temperature stability of KNN-KCN ceramics was better than that of KNN-KCN-Sb ones. Meanwhile, decreasing tendency in relative dielectric constants with increasing measurement frequency observed for all ceramics, shown in Fig 3, which might be attributed to the limited contribution of space charge. For instance, significant differences between dielectric spectrums measured at 1 kHz as compared to those measured at higher frequencies were observed in KNN-KCN-Sb ceramics sintered in air. Dominant defects for KNN-KCN-Sb are highly likely space charges unlike oxygen vacancies. Therefore, it was expected that the oxygen-rich sintering atmosphere, in other words elimination of oxygen vacancies, resulted in decreased concentration of space charges represented by the defect reaction given in Equation 1^{31,33,34}.



According to Kröger-Vink notation in Equation 1, decreasing the concentration of free electrons causes lowering the space charge

density for KNN-KCN-Sb ceramics sintered in the oxygen atmosphere. A similar correlation was observed for dielectric loss values of KNN-KCN-Sb ceramics sintered in oxygen atmosphere, which was 30% lower than that of ceramics sintered in air.

Table 4 shows that comparison of the density and some piezoelectric and dielectric values of KNN-KCN and KNN-KCN-Sb ceramics sintered in oxygen atmosphere with the ones sintered in air or oxygen atmosphere reported in the literature. Incorporation of copper (in the form CuO or KCN) into the KNN resulted in improving the densification together with decreasing the d_{33} values due to inducing hard character. On the other hand, it was found that the relative densities (>99%) for undoped and Sb-doped KNN ceramics were obviously enhanced due to sintering in oxygen atmosphere. However, Sb-doping caused decreasing hard character in KNN-KCN ceramics slightly.

Table 4. Relative Density, piezoelectric constant (d_{33}) and dielectric loss ($\tan \delta$) of samples in comparison with KNN ceramics reported in various literatures.

Composition	Relative Density (%)	Piezoelectric Constant d_{33} (pC/N)	Dielectric Loss @1kHz $\tan \delta$ %	Reference
KNN (air atm.)	94.5	125	-	(35)
KNN-CuO (air atm.)	97.4	83	-	(35)
KNN-KCN (O ₂ atm.)	97.5	180 (pm/V)	1.1	(20)
KNN-KCN (O ₂ atm.)	99.2	80	0.31	This study
KNN-KCN-Sb (O ₂ atm.)	99.4	106	1.3	This study

Fig. 4 shows the Cole-Cole plots of real (Z') vs imaginary (Z'') part of impedance as a function of temperature between 425 and 525°C (at 25°C interval). Fig 4 (a) shows the complex Z' vs Z'' curves belonging to KNN-KCN and KNN-KCN-Sb ceramics sintered in air for 2 h and measured at 500°C. The impedance values of KNN-KCN dramatically decreased with Sb doping. In other words, higher dielectric loss values together with the sharp increments of them especially at temperatures greater than T_d , was probably responsible for the lower impedance behavior observed in KNN-KCN-Sb ceramics.

On the other hand, the comparison of the Z' vs Z'' curves at 500 °C belonging to KNN-KCN-Sb ceramics sintered in different atmospheres were shown in Fig 4 (b). Higher impedance values for KNN-KCN-Sb ceramic sintered under oxygen atmosphere were related to decreasing space charges^{31,36}. Furthermore, increased impedance values were consistent with decreasing dielectric loss values in KNN-KCN-Sb ceramics. Meanwhile, the small semi-circles at lower frequency region in Cole-Cole plots were due to the grain boundary effect. Fig. 4 (c) illustrated impedance plots of KNN-KCN ceramics sintered at different atmospheres as a function of measurement temperatures between 425 and 525°C. Decreases in the radius of semi-circles with increasing temperature highly likely came from the increased activation energy of ionic charge carries. However, the impedance values of KNN-KCN ceramics sintered in air appeared to be higher than those of sintered under oxygen atmosphere. It can be associated with decreasing oxygen

vacancy concentration due to oxygen atmosphere sintering^{25,29}. Similar semi-circles at lower frequencies seen in Fig 4 (c), however, is not very clear like KNN-KCN-Sb which may be associated with hard character in KNN-KCN.

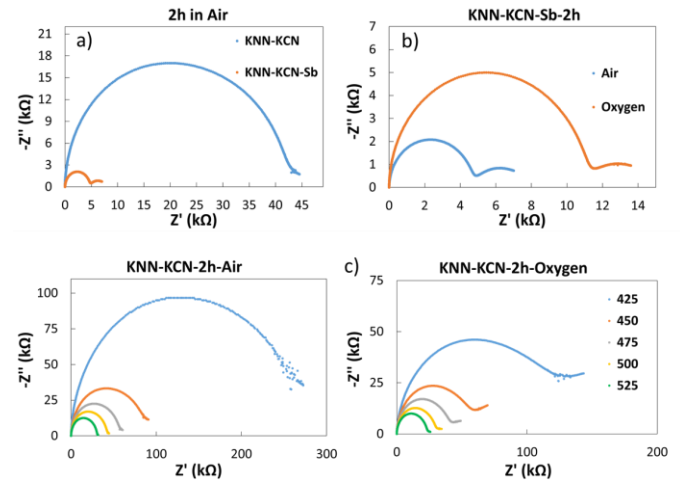


Figure 4. (a) 500 °C Z' vs Z'' curves of KNN-KCN and KNN-KCN-Sb samples sintered in air for 2h (b) 500 °C Z' vs Z'' curves of KNN-KCN-Sb samples sintered in air and oxygen atmosphere for 2h (c) Z' vs Z'' curves of KNN-KCN samples sintered at different atmospheres as a function of measurement temperatures between 425 and 525°C.

4. CONCLUSION

The results of this study may be briefly summarized as follow; sintering in air or oxygen atmosphere did not bring about any significant difference in the XRD patterns of KNN-KCN and KNN-KCN-Sb ceramics. Relative densities of ceramics sintered in an oxygen-rich atmosphere were ~1.5 % higher than those sintered in an air atmosphere. Neither the sintering time nor the sintering atmosphere was found to have any apparent effect on the microstructures of KNN-KCN and KNN-KCN-Sb ceramics. Piezoelectric charge coefficient values were found to be independent of sintering time and/or sintering atmosphere. However, significant increases (~25 %) in the d_{33} values were observed in the presence of Sb doping. Relative dielectric constants and dielectric loss values increased due to Sb doping. T_c and T_d of KNN-KCN system shifted to lower temperatures by ~40 °C in the presence of Sb doping, which obviously decreased the impedance behavior of KNN-KCN ceramics.

Sintering of both ceramic systems in an oxygen-rich atmosphere increased impedance values, especially making the doped lead free environmentally friendly piezoelectric ceramic an alternative candidate to be eligible in high energy density ultrasonic applications.

References

- [1] B. Jaffe, W.R. Cook, H. Jaffe, "Piezoelectric Ceramics." *Academic Press*, New York, (1971).
- [2] K. Uchino, "Piezoelectric Actuators and Ultrasonic Motors." *Springer*, Berlin, (1997).
- [3] A. Halliyal, A. Safari, "Ferroelectrics" **158**, 295 (1994).
- [4] E. K. Akdoğan, A. Hall, W. K. Simon, A. Safari, "Nonlinear dielectric properties and tunability of $0.9\text{Pb}(\text{Mg}_{1/3}\text{Nb}_{2/3})\text{O}_3$ – 0.1PbTiO_3 and $\text{Ba}(\text{Ti}_{0.85}\text{Sn}_{0.15})\text{O}_3$ paraelectrics" *Journal of Applied Physics*, **101**, 024104 (2007).
- [5] G. Robert, M. Demartin and D. Damjanovic, "Phase diagram for the $0.4\text{Pb}(\text{Ni}_{1/3}\text{Nb}_{1/3})\text{O}_3$ – $0.6\text{Pb}(\text{Zr,Ti})\text{O}_3$ solid solution in the vicinity of a morphotropic phase boundary." *Journal of the American Ceramic Society*, **81**, 749-753 (1998).
- [6] W. Yugong, H. Zhang, Y. Zhang, M. Jinyi, X. Daohua, "Lead-free piezoelectric ceramics with composition of $(0.97-x)\text{Na}_{1/2}\text{Bi}_{1/2}\text{TiO}_3$ – 0.03NaNbO_3 – $x\text{BaTiO}_3$ " *Journal of Materials Science*, **38**, 987–994 (2003).
- [7] T.R. Shrout, S.J. Zhang, "Lead-free Piezoelectric Ceramics: Alternatives for PZT?" *Journal of Electroceramics*, **19** (1), 113-126 (2007).
- [8] J. Rödel, K.G. Webber, R. Dittmer, W. Jo, M. Kimura, D. Damjanovic, "Transferring lead-free piezoelectric ceramics into application.", *Journal of the European Ceramic Society*, **35** (6), 1659-1681 (2015).
- [9] RoHS, 2003. European Union Directive, 2002/95/EC, Restriction of the Use of Certain Hazardous Substances in Electrical and Electronic Equipment.
- [10] RoHS, 2011. European Union Directive, 2011/65/EC, Restriction of the Use of Certain Hazardous Substances in Electrical and Electronic Equipment.
- [11] Y. Huan, X. Wang, T. Wei, P. Zhao, J. Xie, Z. Ye, L. Li, "Defect control for enhanced piezoelectric properties in SnO_2 and ZrO_2 co-modified KNN ceramics fired under reducing atmosphere" *Journal of the European Ceramic Society*, **37** (5), 2057-2065 (2017).
- [12] G. Lévêque, P. Marchet, F. Levassort, L.P. Tran-Huu-Hue, J.R. Duclere, "Lead free $(\text{Li,Na,K})(\text{Nb,Ta,Sb})\text{O}_3$ piezoelectric ceramics: Influence of sintering atmosphere and ZrO_2 doping on densification, microstructure and piezoelectric properties." *Journal of the European Ceramic Society*, **31** (4), 577-588 (2011).
- [13] A. Berksoy-Yavuz, U. Basaran, E. Mensur Alkoy, S. Alkoy, "Synthesis of antiferroelectric NaNbO_3 crystals obtained by two-stage molten salt and topochemical crystal transformation processes and their structural characterization." *Afyon Kocatepe University Journal of Science and Engineering*, **14**, OZ5711, 67-71 (2014).
- [14] R. Rai, I. Coondoo, R. Rani, I. Bdikin, S. Sharma, A.L. Kholkin, "Impedance spectroscopy and piezoresponse force microscopy analysis of lead-free $(1-x)\text{K}_{0.5}\text{Na}_{0.5}\text{NbO}_3$ – $x\text{LiNbO}_3$ ceramics." *Current Applied Physics*, **13** (2), 430-440 (2013).
- [15] E. Akça and H. Yılmaz, "Lead-free potassium sodium niobate piezoceramics for high-power ultrasonic cutting application: Modelling and prototyping." *Processing and Application of Ceramics*, **13** (1), 65–78 (2019).
- [16] E. Akça and H. Yılmaz, "Sintering behavior and electrical properties of $\text{K}_4\text{CuNb}_8\text{O}_{23}$ modified $\text{K}_{0.5}\text{Na}_{0.5}\text{NbO}_3$ ceramics with SnO_2 , ZnO or Yb_2O_3 doping." *Ceramics International*, **41** (3), 3659-3667 (2015).
- [17] E. Akça, "Modification of KNN ferroelectric ceramics for high power ultrasonic applications." PhD Dissertation (in Turkish), Gebze Technical University, (2016).
- [18] S. Zhang, H.J. Lee, J. B. Lim, T.R. Shrout, "Characterization of Hard Piezoelectric Lead-Free Ceramics." *IEEE Transactions on Ultrasonics, Ferroelectrics, and Frequency Control*, **56**, 8, (2009).
- [19] J.B. Lim, S. Zhang, H.J. Lee, J.H. Jeon and T.R. Shrout, "Shear-mode piezoelectric properties of modified-(K,Na)NbO₃ ceramics for "hard" lead-free materials." *Journal of the American Ceramic Society*, **93**, 2519-2521 (2010).
- [20] M. Matsubara, T. Yamaguchi, K. Kikuta, S. Hirano, "Sinterability and piezoelectric properties of (K,Na)NbO₃ ceramics with novel sintering aid." *Japanese Journal of Applied Physics*, **43** (10), 7159-7163 (2004).
- [21] N.M. Hagh, B. Jadidian, A. Safari, "Property-processing relationship in lead-free (K, Na, Li) NbO₃ - solid solution system." *Journal of Electroceramics*, **18** (3), 339-346 (2007).
- [22] X. Vendrell and L. Mestres, "Optimization of the sintering conditions of the $[(\text{K}_{0.5}\text{Na}_{0.5})_{1-x}\text{Li}_x]\text{NbO}_3$ system." *Physics Procedia*, **8**, 57-62 (2010).
- [23] P. Palei, M. Pattanaik, P. Kumar, "Effect of oxygen sintering on the structural and electrical properties of KNN ceramics," *Ceramics International*, **38** (1), 851-854 (2012).
- [24] R. Zuo, J. Fu, D. Lv, Y. Liu, "Antimony tuned rhombohedral-orthorhombic phase transition and enhanced piezoelectric properties in sodium potassium niobate." *Journal of the American Ceramic Society*, **93** (9), 2783-2787 (2010).
- [25] H.Y. Park, I.T. Seo, M.K. Choi, S. Nahm, H.G. Lee, H.W. Kang, B.H. Choi, "Microstructure and piezoelectric properties of the CuO-added $(\text{Na}_{0.5}\text{K}_{0.5})(\text{Nb}_{0.97}\text{Sb}_{0.03})\text{O}_3$ lead-free piezoelectric ceramics." *Journal of Applied Physics*, **104** (3), 034103 (2008).
- [26] H. Du, Z. Li, F. Tang, S. Qu, Z. Pei, W. Zhou, "Preparation and piezoelectric properties of $(\text{K}_{0.5}\text{Na}_{0.5})\text{NbO}_3$ lead-free piezoelectric ceramics with pressure-less sintering." *Materials Science and Engineering B*, **131**, (1-3), 83–87 (2006)
- [27] P. Kumar, M. Pattanaik, Sonia, "Synthesis and characterizations of KNN ferroelectric ceramics near 50/50 MPB." *Ceramics International*, **39**, 65–69 (2013).
- [28] M. Matsubara, T. Yamaguchi, W. Sakamoto, K. Kikuta, T. Yogo, S.I. Hirano, "Processing and piezoelectric properties of lead-free (K, Na)(Nb, Ta) O₃ ceramics." *Journal of the American Ceramic Society*, **88** (5), 1190-1196 (2005).



- [29] I.H. Chan, C.T. Sun, M.P. Houng, S.Y. Chu, "Sb doping effects on the piezoelectric and ferroelectric characteristics of lead-free $\text{Na}_{0.5}\text{K}_{0.5}\text{Nb}_{1-x}\text{Sb}_x\text{O}_3$ piezoelectric ceramics." *Ceramics International*, **37** (7), 2061-2068 (2011).
- [30] G. Robert, D. Damjanovic, N. Setter, and A.V. Turik, "Preisach modeling of piezoelectric nonlinearity in ferroelectric ceramics." *Journal of Applied Physics*, **89**, 5067 (2001).
- [31] J. Walenza, J.B. Gibbons, "Effect of annealing atmosphere pO_2 on leakage current in $80(\text{Bi}_{0.5}\text{Na}_{0.5})\text{TiO}_3$ - $20(\text{Bi}_{0.5}\text{K}_{0.5})\text{TiO}_3$ Piezoelectric Thin Films." *Applied Physics Letters*, **110**, 162904 (2017).
- [32] L. Haimin, Q. Chunli, Z. Jianguo. H. Mingzhe, Y. Qingsong, "Effect of different annealing atmosphere on ferroelectric properties of 0.7BiFeO_3 - 0.3PbTiO_3 thin films." *Rare Metal Materials and Engineering*, **45**, 1449-1454 (2016).
- [33] N. Kumar and D.P. Cann, "Tailoring transport properties through nonstoichiometry in BaTiO_3 - BiScO_3 and SrTiO_3 - $\text{Bi}(\text{Zn}_{1/2}\text{Ti}_{1/2})\text{O}_3$ for capacitor applications." *Journal of Materials Science*, **51**, 9404-9414 (2016).
- [34] A. Podpirka, B. Viswanath, and S. Ramanathan, "Active low temperature oxidation as a route to minimize electrode-oxide interface reactions in nanoscale capacitors." *Journal of Applied Physics*, **108**, 024106 (2010).
- [35] Wang, T, Liao, Y, Wang, D, et al. "Cycling- and heating-induced evolution of piezoelectric and ferroelectric properties of CuO-doped $\text{K}_{0.5}\text{Na}_{0.5}\text{NbO}_3$ ceramic." *J Am Ceram Soc*, **102**, 351– 361 (2019).
- [36] C. Long, T. Li, H. Fan, Y. Wu, L. Zhou, Y. Li, L. Xiao, Y. Li, "Li-substituted $\text{K}_{0.5}\text{Na}_{0.5}\text{NbO}_3$ -based piezoelectric ceramics: Crystal structures and the effect of atmosphere on electrical properties." *Journal of Alloys and Compounds*, **658**, 839-847 (2016).